

## Fabrication and Characterization of Gold Nano-gaps for ssDNA Immobilization and Hybridization Detection

Th.S. Dhahi<sup>1</sup>, U. Hashim<sup>1</sup>, N.M. Ahmed<sup>2</sup> and H. Nazma<sup>1</sup>

<sup>1</sup>Institute of Nano Electronic Engineering, University Malaysia Perlis (UniMAP)

<sup>2</sup>University Sains Malaysia (USM), Malaysia

Received: November 10, 2010, Accepted: December 16, 2010, Available online: May 13, 2011

**Abstract:** We develop a method for fabricating the nano-gaps directly by using just photolithography and wet etching processes without any nano lithography or difficult techniques. It shows that this resolution enhancement allows one to fabricate metal electrodes with separation from arbitrarily large to fewer than one hundred nanometers. Furthermore, because these nano-gaps are on a thin film, they can be imaged with high-resolution transmission electron microscopy (HRTEM). Efforts toward achieving electrical contact to nanostructures have been active for over a decade. Even though several devices based on “nano-gaps” – two gaps separated by a nanometer-scale distance - have been demonstrated, their realization has remained a significant challenge. Even the best methods are highly labor-intensive and suffer from low yield and poor geometrical control. Most nano-gaps are also incompatible with high resolution transmission electron microscopy (HRTEM) and scanning electron microscopy (SEM). As a consequence, the proof of the nano-gap quality and content in past studies has been indirect. High-resolution imaging is therefore required to ensure the quality of nano-gaps and to be able to identify possible artifacts. This project presents a unique vertical nano-gap biosensor that can detect changes in DNA structure. Using a size reduction to interrogate samples between the nano-scale gaps, this biosensor will be sensitive enough to record the conformational changes for ss-DNA.

**Keywords:** Nano-gap, biosensor, DNA, Gold Electrode, Immobilization, Hybridization.

### 1. INTRODUCTION

In the past two decades, nano-fabrications have seen great advances in the development of biosensors and biochips for characterizing and quantifying biomolecules. Nanofabrication techniques are progressively being applied to create sensors of ultra-miniature size. The reduction in sensor size can result in lower material costs, reduced weight, and lower power consumption, which are the key factors driving opportunities for sensors in the marketplace. Nano-sensors of highly reduced power consumption are very suitable for integration into wireless communication devices to enable widespread distributed monitoring and control. Very low-power nano-sensors would also be beneficial for use as battery-operated handheld or wearable sensors. Logical and promising sensing application areas for nano-sensors include medical (e.g., blood gas monitoring/blood analysis, patient monitoring, diagnostic testing), biowarfare detection, genetic analysis, drug

discovery, food inspection/testing, environmental monitoring, and industrial chemical processes monitoring leak detection.

Figure 1 shows TEM images of examples of nano-gaps on Si<sub>3</sub>N<sub>4</sub> membranes with gap sizes of 0.7, 1.5, 3, 4, 5 and 6 nm (Fig 1 (a-f), respectively). A HRTEM image of another 4 nm gap is also shown (Fig. 1 (g)) [1].

Recently, there has been growing interest in DNA biosensors due to its significant detection properties [2-10]. One of the most popular applications of the new devices was detection and analysis of specific DNA sequences via nucleic acid hybridization [11-20]. Fast and reliable determination of nucleic acid sequences plays an increasingly important role in clinical diagnosis, forensic and environmental analyses, and food safety monitoring [21-25]. Conventional methods are often time-consuming and expensive, therefore new DNA hybridization-based biosensors have received considerable attention [23, 24, 26]. The detection layer of the biosensor consists of short single-stranded DNA (ssDNA probe) able to form a duplex with a complementary target nucleic acid fragment with

\*To whom correspondence should be addressed: Email: sthikra@yahoo.com  
Phone:

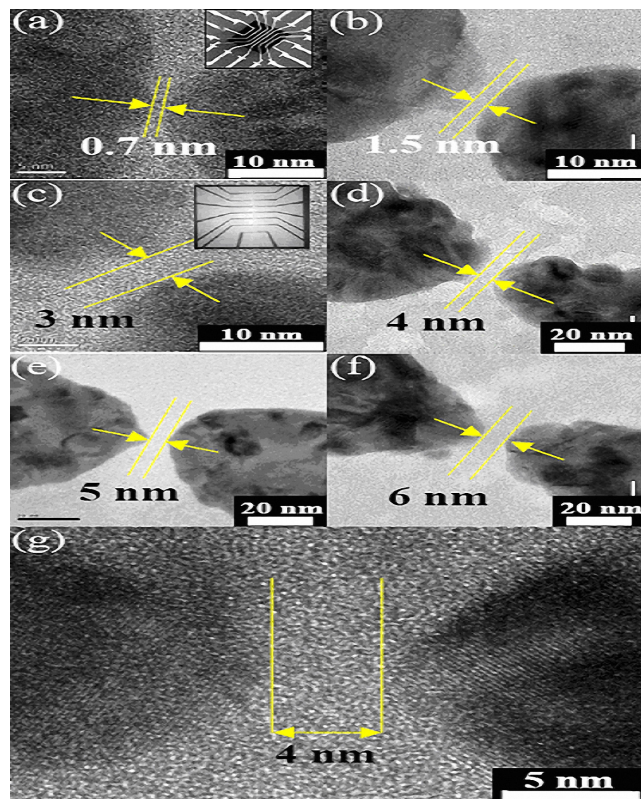


Figure 1. TEM image of nano-gaps with sizes 0.7 nm (a), 1.5 nm (b), 3 nm (c), 4 nm (d), 5 nm (e) and 6 nm (f). (g) HRTEM image of another 4 nm nano-gap. The crystal lattice planes of the electrodes (g) are seen clearly. Inset to (a): SEM image of a full device consisting of electrodes (white lines) on a suspended  $50\ \mu\text{m} \times 50\ \mu\text{m}$   $\text{Si}_3\text{N}_4$  membrane (black square) and connected to larger wires. Inset to (c): TEM image of electrodes (black lines) on a suspended  $\text{Si}_3\text{N}_4$  membrane.

high efficiency and specificity. The probe is attached to a transducer that translates the hybridization event into a physically measurable signal [19, 27, 28]. Among different combinations of ssDNA probes and transduction elements the electrochemical DNA biosensors show very useful analytical abilities. They have relatively simple construction, are not expensive, enable appropriately sensitive and selective detection of target DNA fragments, and can be used for routine tests [4, 10, 13, 17, 22, 28].

The fabrication and characterization of nano-structures are given and developed in this work using a photolithography process and wet etching for the gold layer to form the nano-gaps. Chrome masks are used to fabricate the nano-gap structure using gold material to increase the conductivity and the selectivity with the biosensor detection process, so a very simple process for nano-fabrication is submitted in this work to consume both the time and the cost with any expensive technology.

## 2. EXPERIMENTAL METHOD

### 2.1. Nano-gap Biosensor Mask Design

The use of nano-gaps has allowed the introduction of many new

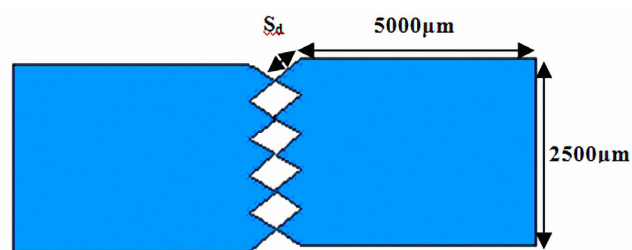


Figure 2. Design Specification of the mask

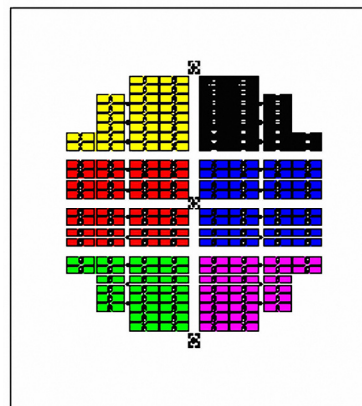


Figure 3. Schematic design of the actual mask on chrome glass

signal transduction technologies in biosensors. The sensitivity and performance of biosensors is being improved by using a doping process for their construction.

The starting material is an N-type, 100mm in diameter silicon substrate. As for the lithography process, one photomask is used to fabricate the nanogap using conventional photolithography coupled with wet etching processes. A chrome mask is used here for better results. This mask is used to develop and form a gold nano-gap. The photomask is designed using AutoCAD software and then printed onto a chrome glass surface.

Figure 2 is the mask for nanogap electrode formation with a length and width of  $5000\ \mu\text{m}$  and  $2500\ \mu\text{m}$ , respectively.

The proposed angle length of the end electrode is shown in Table 1. This is simply to check the best angle for the best nanogap formation after the etching process.

The symbol  $S_d$  refers to the dimension for the side angle of the

Table 1. Difference in dimensions for  $S_d$ .

$S_d$	$\mu\text{m}$
1	1100
2	1000
3	900
4	800
5	700
6	600

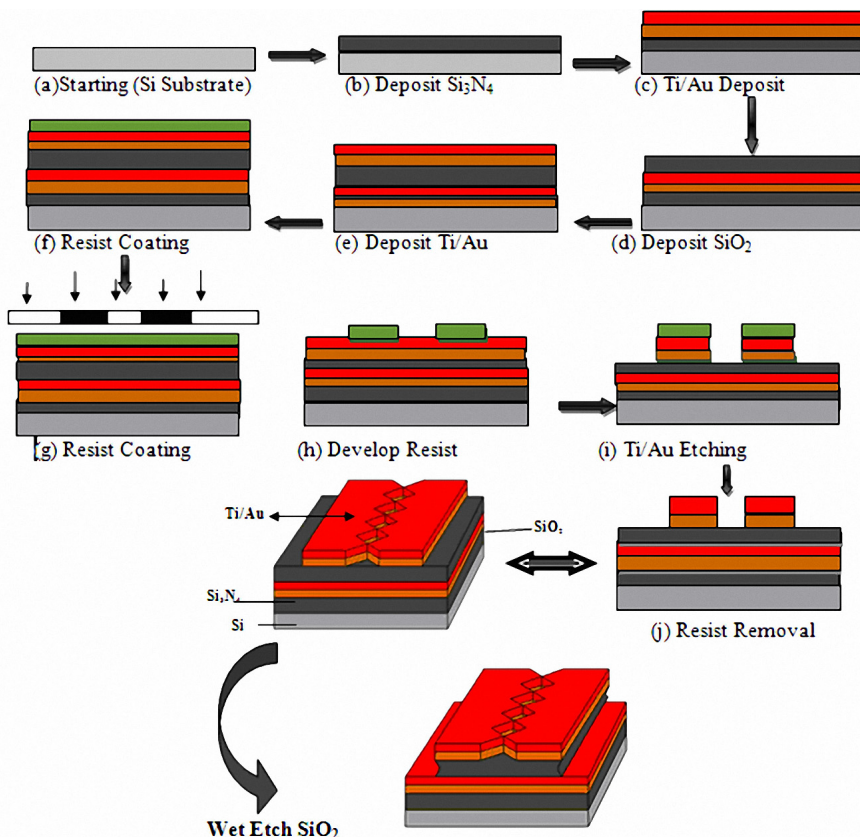


Figure 4. Gold/Ti-Silicon nano-structure pattern process flow

design for nano-gap formation. It shows that when  $S_d$  is large this means the gap becomes very sharp, and on the other hand the gap is less sharp when  $S_d$  is reduced.

Figure 3 shows a complete arrangement of mask design with different gap sizes on the chrome glass.

In the actual mask the total device is 160 devices, and the length and width for each electrode in each device is 5000 $\mu\text{m}$  and 2500 $\mu\text{m}$ , respectively.

The diameter for the wafer is four (4) inches, each device has five nano-gaps, and the dimension of the gap for each device is different for each one.

## 2.2. Device Fabrication

The detailed process flow of gold nano-gap fabrication is shown in Figure 4. First, a  $\text{Si}_3\text{N}_4$  layer is deposited onto the silicon substrate as we can see in Figure 4(a). Then, before continuing with silicon oxide deposition, a layer of Ti/Au is deposited on the  $\text{Si}_3\text{N}_4$  surface layer. For the photolithography process, a positive photo resist is used to coat onto the gold surface, and then UV exposed through Mask1. After development, only unexposed resist will remain on the sample. Figure 4(i) shows the resist pattern after the development process. The Ti/Au layer is etched before removing the resist layer. Then the wet etching for the  $\text{SiO}_2$  layer is performed and the final structure of the nano-gap gold electrode fabrication is obtained as shown in Figure 4.

## 3. RESULTS AND DISCUSSIONS

Figure 5 shows the chrome glass for the actual mask.

Chrome glass contains 6 sets of different designs in  $S_d$ , where each group contains a certain measure of  $S_d$ , since the right side and left side of the face on top are 1100 $\mu\text{m}$  and 600 $\mu\text{m}$ , respectively, while the left and right side of the center are 1000 $\mu\text{m}$  and 900 $\mu\text{m}$ , respectively, and 800 $\mu\text{m}$  and 700 $\mu\text{m}$  to the left and right side of the bottom of the chrome glass.

In the chrome glass the total device is 160 devices, the length and width for each electrode in each device is 5000 $\mu\text{m}$  and 2500 $\mu\text{m}$ , respectively. The diameter of the chrome glass is 4 inches, each device has five nano-gaps, and the dimension of the gap for each device is different for each one.

Figure 6 shows a micrograph image of the pattern on the Si wafer after the developing process.

From Figure 5 we can see the early un-joined gap.

After the retransfer process for the nano-structure on the chrome mask glass to correct the wrong design, we can see this in Figure 7, which includes the SEM image for the correct structure on the chrome mask to fabricate the gold nano-gaps later using a wet etching process for the gold layer, by using an aqua regia solution.

The chrome mask is the important step in our project to fabricate and develop the nano-structure using a photolithography process [29], so the novelty in this work is in assigning a simple process to create the pattern for the nanogaps [30], with a wet-etching process using a chemical solution to form the gold nanostructure as seen in Figure 8.

## 4. PLAN FOR FUTURE BIOSENSOR FABRICATION

### 4.1. DNA Immobilization and Hybridization

A bis-intercalator echinomycin (ECHI) and a simple intercalator  $[\text{Co}(\text{phen})_3]^{3+}$  were used as novel electrochemical redox indicators to detect DNA hybridization at gold electrodes (AuE). In order to minimize the nonspecific adsorption of oligonucleotides (ODN), the thiol-derivatized oligonucleotides were immobilized onto the AuE in the first step, and the exposition of AuE to 6-mercapto-1-hexanol (MCH) followed in the second step of this procedure. In this arrangement good reproducibility and discrimination between single-stranded (ss) probes and double-stranded (ds) hybrid DNA were obtained. While both redox indicators showed a good ability to discriminate between the ss probe and the ds hybrid DNA, the signals of ECHI were by an order of magnitude higher than those of  $[\text{Co}(\text{phen})_3]^{3+}$  in a good agreement with stronger DNA binding by the bis-intercalator as compared to the simple intercalator. In addition, DNA single-base mismatch (DNA point mutation) was

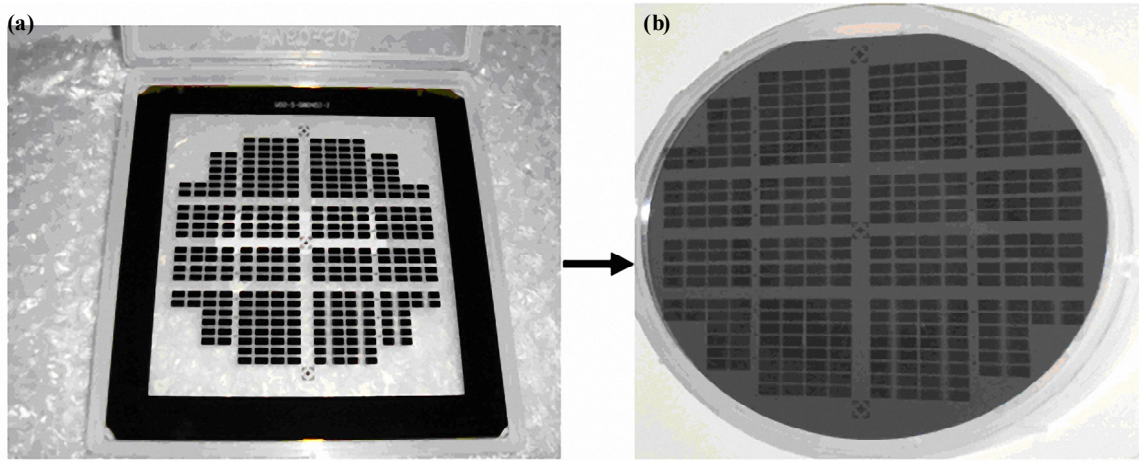


Figure 5. (a) The actual mask in chrome glass, (b) Si wafer after the exposure process

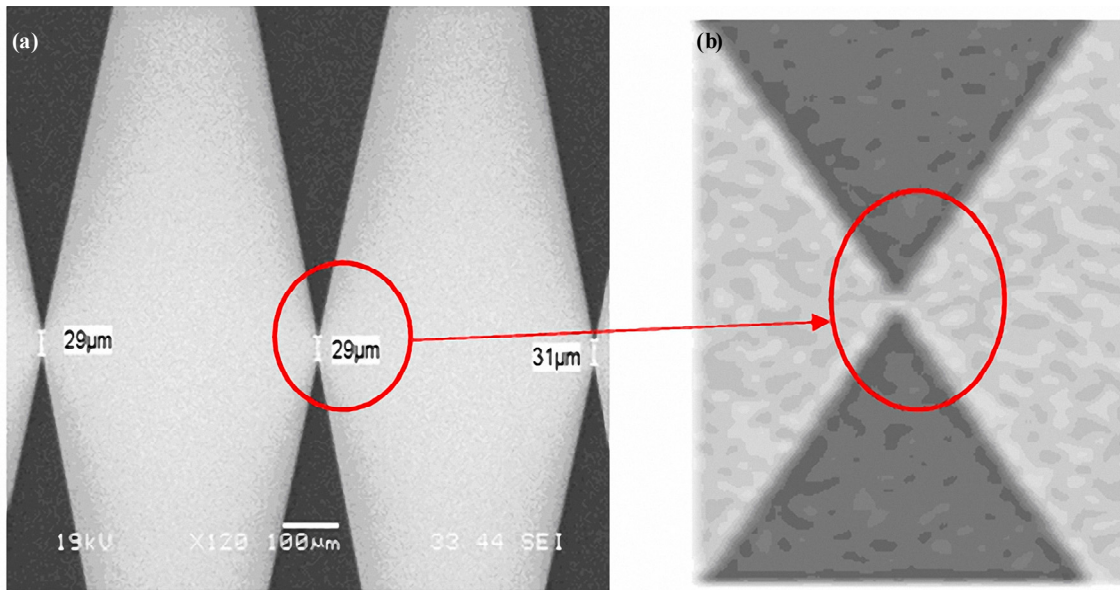


Figure 6. SEM micrograph shows the nano-gap is un-joined. (a) Image gap as 19 kx, (b) Image gap as 25 kx

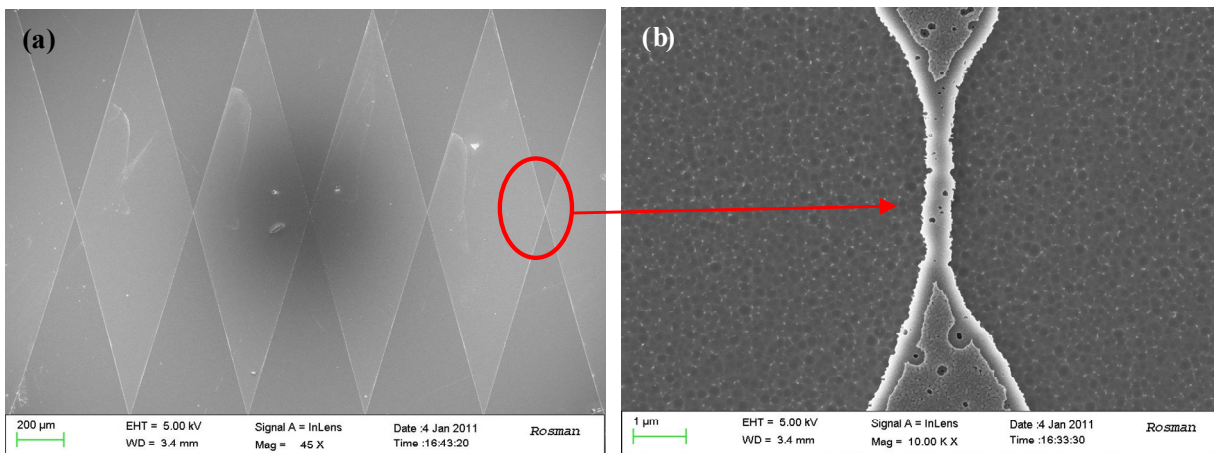


Figure 7. SEM images for the nano-gaps with: (a) Magnification 45X, (b) Magnification 10.00 KX

easily detected by means of ECHI [30].

#### 4.2. Electrode pretreatment

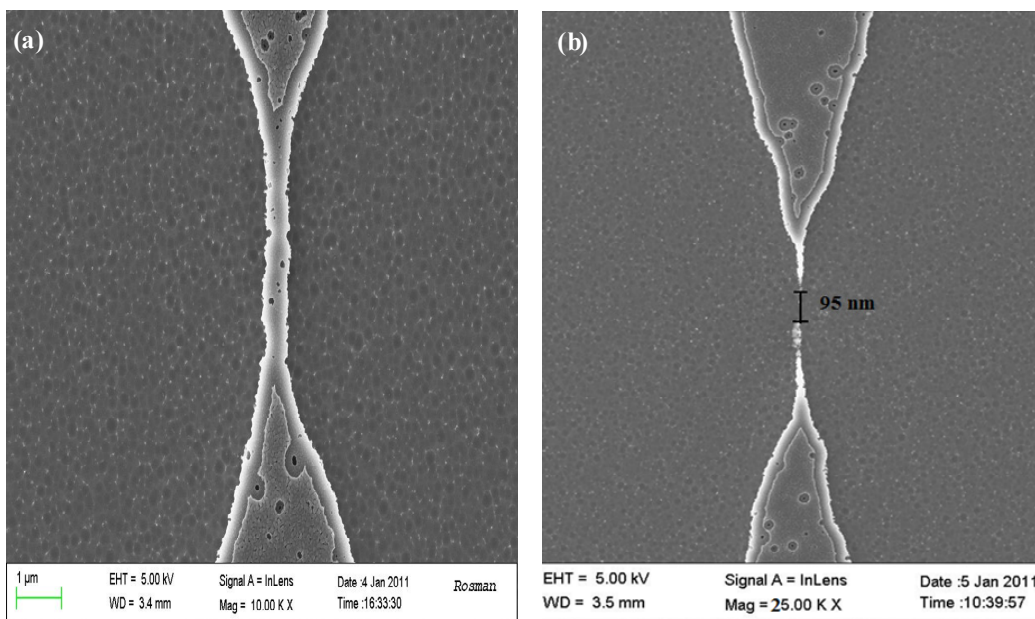


Figure 8. SEM images for the nano-gap fabrication: (a) before wet-etching processes, (b) after wet-etching processes

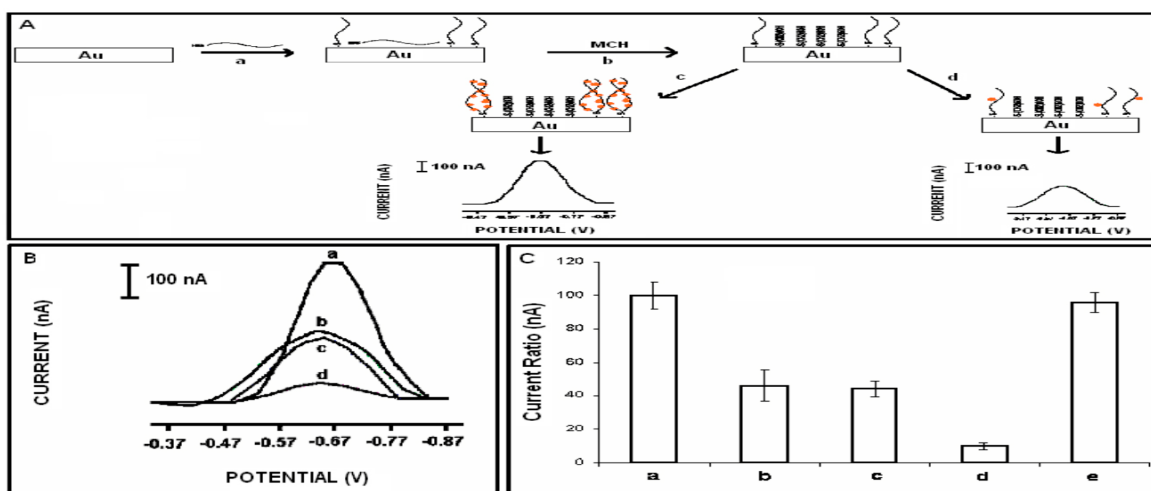


Figure 9. A Scheme representing electrochemical detection of DNA hybridization with a bis-intercalator ECHI (a) SH-linked probe immobilization onto a gold electrode (AuE) surface, (b) addition of 0.1 mM MCH in order to provide a better surface, (c) electrochemical measurement based on ECHI signal, after binding of ECHI to DNA hybrid (between probe and complementary), (d) electrochemical measurement based on ECHI signal, after binding of ECHI to DNA probe. B. Differential pulse voltammograms of ECHI: (a) hybridization of the probe P1 with complementary strand T1, (b) probe P1 alone, (c) hybridization of the probe P1 and non-complementary strand (d) bare electrode. C. Histograms for the relative reduction signals of ECHI obtained: (a) after hybridization of the probe P1 with complementary strand T1, (b) probe P1 alone, (c) hybridization of the probe P1 and non-complementary strand (d) bare electrode, (e) hybridization between probe and complementary T1 in the presence of non-complementary strand in an equal ratio (1:1) [30].

The AuE surface was prepared for modification by polishing with a 0.1 μm alumina/water slurry on a polishing cloth for 5 minutes and it was sonicated for 5 min. The electrode was then cleaned by using a cyclic voltammetry procedure in the potential range of -0.9 and +0.9 V in 0.05M H<sub>2</sub>SO<sub>4</sub> solution at a scan rate of 150 mV/sec until reproducible curves were recorded. The electrode was

rinsed with distilled water for 5 seconds before probe immobilization. The AuE SAM modification and the detection of hybridization were performed as shown in Figure 7A.

### 4.3. Thiol-linked probe immobilization onto the surface of the gold electrode

Probe immobilization onto the AuE pretreated surface was performed as follows: The AuE was inverted and 20  $\mu\text{L}$  of 10  $\mu\text{g}/\text{ml}$  thiol-linked probe in a 0.5 M acetate buffer solution, with a pH of 4.80 (ABS), was pipetted onto the surface of the AuE. The droplet was air-dried for 3 hours. It was then rinsed with ABS for 10 seconds to remove any unbound ODN material.

SAM was prepared by the immersion of the probe-modified AuE in freshly prepared 75 : 25 (v/v) ethanol : water solution containing 0.1mM MCH. AuE was incubated in this ethanolic solution for 1 hour. The AuE / SAM was rinsed with 75:25 (v/v) ethanol : water.

### 4.4. Hybridization

For detection of hybridization, after the immobilization of the thiol-linked probe, the probe-modified AuE was inverted and 20  $\mu\text{L}$  of 15  $\mu\text{g}/\text{ml}$  complementary or non-complementary or mismatched DNAs in a 20 mM Tris buffer solution with a pH of 7.0 (TBS) was pipetted onto the surface. The target droplet was air-dried for 1 hour. It was then rinsed with TBS for 10 seconds to remove any unbound ODN material.

## 5. CONCLUSIONS

The aim of this research is to develop the chrome mask to fabricate the nano-gap structure and apply it in the biosensor for specific DNA sequences, using synthetic single-stranded DNA as a model system. A conductance-based sensor for the direct detection of DNA fabrication and sequences is described. Hybridization of target DNA with immobilized DNA between the nano-gap induces charge effects, altering the electrical properties of the bio-layer, and can be detected by the associated change in the measured conductance and capacitance, which is monitored electronically by using a semiconductor parameter analyzer, spectroscope and oscilloscope. Using the electrical detection mechanism of a nano-gap sensor promises fast and direct real-time monitoring of DNA hybridization of DNA without being time-consuming and at low cost. DNA change from single-stranded DNA (ssDNA) to double-stranded DNA (dsDNA) in the hybridization process causes the change of charge density of the tested molecular structure. SEM images are used to investigate the nano-gap structures and DNA as a target in future work.

## 6. ACKNOWLEDGMENT

This work was supported by the Institute of Nano Electronic Engineering (INEE) University Malaysia Perlis (UniMaP) and the Faculty of Science, University Putra Malaysia.

## REFERENCES

- [1] Michael D. Fischbein and Marija Drndic, *Nano Lett.*, 5, 549 (2005).
- [2] Wang, J., Rivas, G., Cai, X., Palecek E., Nielsen P., Shiraishi H., Dontha N., Luo D., Parrado C., Chicharro M., Farias P.A.M., Valera F.S., Grant D.H., Ozsoz M., Flair M.N., *Anal. Chim. Acta*, 347, 1 (1997).
- [3] Marrazza G., Chianella I., Mascini M., *Anal. Chim. Acta*, 387, 297 (1999).
- [4] Mascini M., Palchetti I., Marrazza G., *J. Anal. Chem.*, 361, 15(2001).
- [5] Hall R.H., *Microbes Infect*, 4, 425 (2002).
- [6] Palecek E., Jelen F., *Critical Rev. Anal. Chem.*, 32, 261 (2002).
- [7] Drummond T.G., Hill M.G., Barton J.K, *Nature Biotech.*, 21, 1192 (2003).
- [8] de-los-Santos-Álvarez P., Lobo-Castañón M.J., Miranda-Ordieres A.J., Tuñón-Blanco P. *Electroanalysis*, 16, 1193 (2004).
- [9] Bakker E., Qin Y., *Anal. Chem.*, 78, 3965 (2006).
- [10] Minunni M., Tombelli S., Mariotti E., Mascini M., Mascini M., *J. Anal. Chem.*, 369, 589 (2001).
- [11] Marrazza G., Chianella I., Mascini M., *Biosens. Bioelectron.*, 14, 43 (1999).
- [12] Pividori M.I., Merkoçi A., Alegret S., *Biosens. Bioelectron.*, 15, 291 (2000).
- [13] Wang J., *Nucleic Acids Res.*, 28, 3011 (2000).
- [14] Xu Ch., He P., Fang Y., *Anal. Chim. Acta*, 411, 31 (2000).
- [15] Watterson J., Piuñno P.A.E., Krull U.J., *Anal. Chim. Acta*, 469, 115 (2002).
- [16] Kerman K., Kobayashi M., Tamiya E., *Meas. Sci. Technol.*, R1-R11, 15 (2004).
- [17] Loaza Ó.A., Campuzano S., López-Berlanga M., Pedrero M., Pingarrón J.M., *Sensors*, 5, 344 (2005), *Sensors*, 8, 2133 (2008).
- [18] Palecek E., Fojta, M. In. *Bioelectronics*, Willner, I., Katz, E., Ed., WILEY-VCH Verlag GmbH & Co, KGaA: Weinheim, 2005, pp 127-192.
- [19] Odenthal K.J., Gooding J.J., *Analyst*, 132, 603 (2007).
- [20] Luong J.H.T., Bouvrette P., Male K.B., *TIBTECH*, 15, 369 (1997).
- [21] Wang J., *Chem. Eur. J.*, 5, 1681 (1999).
- [22] Schmidt A., Bilitewski U., In. *Instrumentation and sensors in the food industry*, Kress-Rogers, E., Brimelov, C.J.B., Ed., Woodhead Publishing Limited: Cambridge, 2001, pp 714-739.
- [23] Nakamura H., Karube I., *Anal. Bioanal. Chem.*, 377, 446 (2003).
- [24] Elenis D.S., Kalogianni D.P., Glynou K., Ioannou P.C., Christopoulos T.K. *Anal. Bioanal. Chem.*, 2008, Epublished ahead of print.
- [25] Hahn S., Mergenthaler S., Zimmermann B., Holzgreve W., *Bioelectrochemistry*, 67, 151 (2005).
- [26] Wang J., *Anal. Chim. Acta*, 469, 63 (2002).
- [27] de-los-Santos-Álvarez P., Lobo-Castañón M.J., Miranda-Ordieres A.J., Tuñón Blanco P., *Anal. Bioanal. Chem.*, 378, 104 (2004).
- [28] Mingqiang Yi, Ki-Hun Jeong, Luke P. Lee, *Biosensors and Bioelectronics*, 20, 1320 (2005).
- [29] Th.S. Dhahi, U. Hashim, N.M. Ahmed, A. Mat Taib., *Journal of Optoelectronics and Advanced Materials*, 12, 1857 (2010).
- [30] Hakan Karadeniz, Beste Gulmez, Arzum Erdem, Frantisek Jelen, Mehmet Ozsoz and Emil Palecek, *Frontiers in Bioscience*, 11, 1870 (2006).